

Bifurcation length in the numerical simulation of the modulation instability

Agissilaos G. Athanassoulis* and Irene Kyza

Department of Mathematics, University of Dundee

Thursday 1st June, 2023

Abstract

The role of modulation instability (MI) in oceanic rogue waves has been hotly debated for years. The onset of instability has been predicted when the wave power spectrum becomes too narrow, but numerical investigations of this have produced mixed results. In this work we identify a clear reason why instability is suppressed in many simulations. Indeed, simulations are performed on a bounded computational domain of characteristic length L with periodic boundary conditions. Here we show for the first time that there exists a bifurcation length $L_c = O(\lambda_0^2)$, below which no MI whatsoever is present. The analysis is carried out on the level of the nonlinear Schrödinger equation (NLS) both for plane waves and for more general power spectra, and is complemented by numerical results. This result highlights the *non-local* character of the MI. Moreover, it establishes the need for computational domains in the *hundreds* of wavelengths λ_0 , if we are to meaningfully investigate the onset of MI in water waves. This fundamental scaling of the MI captured here is expected to carry over to the full water wave equations for quasi-unidirectional problems.

Keywords: Nonlinear Schrödinger equation, Modulation instability, bifurcation, water waves, scientific computing

1 Introduction

The role of MI in oceanic rogue waves has been the topic of vigorous debate, with theses ranging from polemical [6, 15] to circumspect [24, 25, 28, 14, 22, 27]. Of course the classical MI [29] strictly speaking refers only to plane waves, a factor that often exacerbates the confusion. To address that, a linear stability analysis for moments of stochastic wavefields has been carried out in analogy to the classical MI, [1, 13, 23, 2, 3]. This analysis predicts a generalized MI whenever the waves' power spectrum becomes narrow enough, and stabilization through Landau damping whenever the spectrum becomes broad enough. While Landau damping was proved rigorously only recently [3], the physical intuition behind it is sound and consistent with empirical knowledge; indeed, narrower spectra are widely considered “more nonlinear” than broader spectra. However, an abrupt onset of the generalized MI is often not detected in simulations. Only a handful of works find clear evidence for onset of instability at some critical peakedness of the spectrum [23, 26, 5]. In contrast, in many cases the onset of MI is clearly not present in simulations – even in problems where MI has been predicted and is expected [18].

While trying to understand this, we naturally came upon the question “how many wavelengths long must the computational domain be in order for the MI to be well resolved?” Many colleagues that we approached with the question answered that typically 10–20 wavelengths are used in simulations, and that

*Corresponding author email: aathanassoulis@dundee.ac.uk

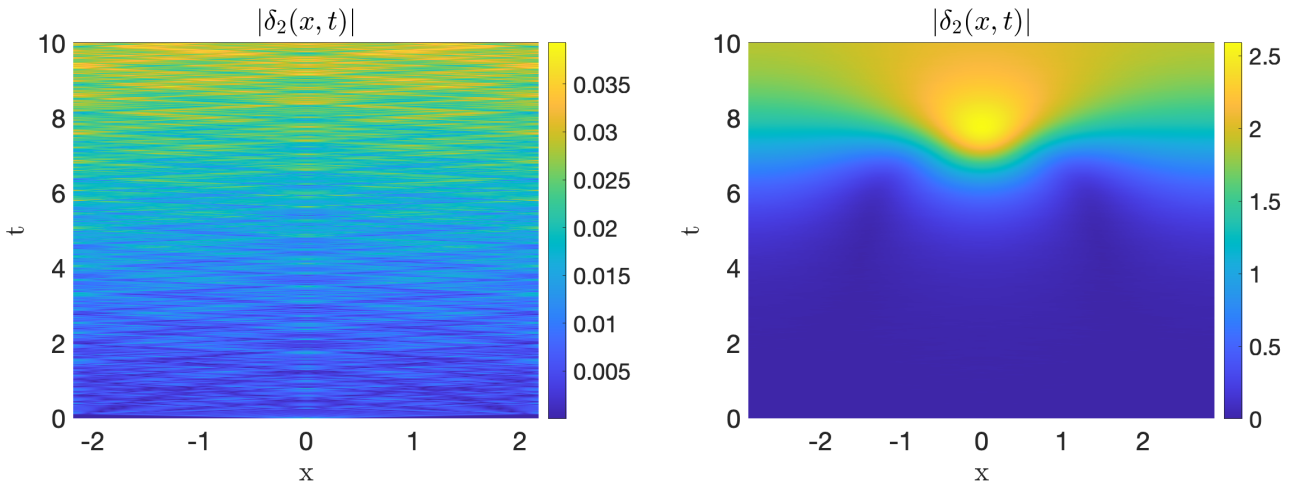


Figure 1: Space-time plot of the modulus of the inhomogeneity, $|\delta_2(x, t)|$, when propagated on intervals of different length L according to equations (17) – (19). Growth of the inhomogeneity to $O(1)$ is evidence of MI. The bifurcation length L_c is reported in equation (15). **Left:** $L = 0.98L_c$. **Right:** $L = 1.3L_c$.

this is widely accepted as enough. However, it turns out that this is a question that can be investigated analytically and answered quantitatively. In Section 2 we redo the stability analysis of plane waves on an interval of length L instead of the real line. It turns out that in a domain shorter than $L_c = C\lambda_0^2$ there is no MI and plane waves are always linearly stable. Since wavelengths of hundreds of meters are typical in ocean waves, this scales the problem to require *hundreds* of wavelengths before the MI is even possible for plane waves. In Section 3, we see that this idea can be applied to stochastic wavefields as well: we carry out the stability analysis of a stochastic wavefield on an interval of length L instead of the real line. We find results analogous to the real line, and a Penrose-type stability condition that contains explicitly the length L . Numerical investigation of the stability condition indicates again the stabilization of MI for short computational domains, even for very narrow spectra.

It must be noted that all the investigations that did detect the onset of MI [26, 5, 23] used 100 wavelengths-long computational domains or longer. Moreover, in the most famous paper reporting no evidence of onset of MI, [19], we could not find a discussion for the size of the computational domain. These findings highlight that the MI is a *non-local phenomenon*, and requires large enough computational domains in order to manifest. Thus, it seems possible that MI is inadvertently suppressed in many state of the art simulations, as often too short computational domains are used.

The paper is organized as follows: in Section 2 we investigate the classical MI and the role of the length L of the interval both analytically and numerically. The abrupt bifurcation between $L < L_c$ and $L > L_c$ is clearly seen in Figure 1. In Section 3 a similar analysis is carried out for the second moments of a stochastic wavefield on $[-\frac{L}{2}, \frac{L}{2}]$ in the spirit of [1, 3]. An instability condition is derived, and solved for a simple case. The results indicate an analogous behaviour, i.e. stabilization of the problem when L is small, even for very narrow spectra. The overall conclusions are discussed in Section 4.

2 Classical MI on the real line and an interval of length L

2.1 On the real line

We briefly go through the standard MI calculation on the real line. This will prepare the ground for the subsequent analysis on a bounded interval. Consider the NLS

$$i\partial_t u + p\Delta u + q|u|^2 u = 0, \quad x \in \mathbb{R}, \quad \sup_{x \in \mathbb{R}} |u(x, t)| < \infty. \quad (1)$$

Equation (1) is known to be well-posed in Zhidkov spaces [16, 30]; this is the natural framework for this discussion. Also, since we are dealing with the focusing NLS, we will assume without loss of generality that $p, q > 0$. Moreover, equation (1) admits the exact solution

$$w(x, t) := Ae^{iqA^2t}, \quad (2)$$

which is the simplest plane wave solution with amplitude $A > 0$. To study the stability of this plane wave solution one can consider whether small perturbations grow. This leads to the perturbed initial value problem

$$i\partial_t u + p\Delta u + q|u|^2u = 0, \quad u(x, 0) = A(1 + \delta_0(x)) \quad (3)$$

for some initial perturbation $\delta_0(x)$ which is small in an appropriate sense, $\delta_0 = o(1)$. Using the substitution

$$u(x, t) = Ae^{iqA^2t}(1 + \delta(x, t)) \quad (4)$$

one readily computes that problem (3) is equivalent to

$$i\delta_t + p\Delta\delta + qA^2(\delta + \bar{\delta}) + qA^2(\delta + \bar{\delta})\delta + qA^2|\delta|^2(1 + \delta), \quad \delta(x, 0) = \delta_0(x). \quad (5)$$

Dropping higher order terms, we obtain the linearized problem for the perturbation, namely

$$i\delta_t + p\Delta\delta + qA^2(\delta + \bar{\delta}), \quad \delta(x, 0) = \delta_0(x). \quad (6)$$

By expanding equation (6) into its real and imaginary parts, and denoting

$$\delta(x, t) = \alpha(x, t) + i\beta(x, t), \quad (7)$$

we eventually obtain the system

$$\partial_{tt}\beta + (p^2\Delta\Delta + 2pqA^2\Delta)\beta = 0, \quad \partial_t\alpha + p\Delta\beta = 0. \quad (8)$$

This now can be solved explicitly with separation of variables, leading to the construction of the modes

$$\zeta \in \mathbb{R}, \quad \beta_\zeta(x, t) = e^{i[\zeta x + \omega(\zeta)t]} + c.c., \quad \omega^2(\zeta) = \zeta^2[p^2\zeta^2 - 2pqA^2]. \quad (9)$$

(Here c.c. stands for complex conjugate.) More general solutions can be formed by superpositions of these modes, $\beta(x, t) = \int M(\zeta)\beta_\zeta(x, t)d\zeta$. The instability is due to the fact that,

$$|\zeta| < A\sqrt{2\frac{q}{p}} \implies \omega(\zeta) = \pm i|\omega(\zeta)| \quad (10)$$

and thus the corresponding modes $\beta_\zeta(x, t)$ of equation (9) contain an exponentially growing component. Therefore the solution δ of the linearized equation (6) generally grows exponentially in time, i.e. the plane wave solution of the NLS is linearly unstable. Moreover the unstable wavenumbers and their rate of growth follow from this analysis.

In this problem there are three parameters, p, q, A . However by rescaling the problem according to $\tau = qA^2t$, $\chi = A\sqrt{\frac{q}{p}}x$, $U(\chi, \tau) = \frac{1}{A}u(x, t)$, the equation is mapped to the ‘‘canonical’’ NLS $i\partial_\tau U + \partial_{\chi\chi}U + |U|^2U = 0$, which has the plane wave solution $W(\chi, \tau) = e^{i\tau}$. That is, the exact values of p, q, A don’t play an important role and the nature of the modulation instability is the same for any $p, q, A > 0$. This widely understood universality of the MI may have contributed to an implicit expectation that the periodized problem enjoys similar properties.

2.2 On an interval of length L

Now let us consider the NLS equation on an interval of length L equipped with periodic boundary conditions,

$$\begin{aligned} i\partial_t u + p\Delta u + q|u|^2 u &= 0, & x \in [-\frac{L}{2}, \frac{L}{2}], \\ u(-\frac{L}{2}, t) &= u(\frac{L}{2}, t), & \partial_x u(-\frac{L}{2}, t) = \partial_x u(\frac{L}{2}, t). \end{aligned} \quad (11)$$

The steps described above in equations (2)-(8) were carried out with boundary conditions of boundedness at infinity; however, one readily checks that each step is equally valid with the periodic boundary conditions on $[-L/2, L/2]$. Indeed, the plane wave is still a solution, the algebra leading to (5) is the same, and finally the linearization and separation of real and imaginary parts are the same. So now we have to solve the problem

$$\partial_{tt}\beta + (p^2\Delta\Delta + 2pqA^2\Delta)\beta = 0, \quad \beta(-\frac{L}{2}, t) = \beta(\frac{L}{2}, t), \quad \partial_x\beta(-\frac{L}{2}, t) = \partial_x\beta(\frac{L}{2}, t). \quad (12)$$

This is the first time that the parameter L really comes into play, and separation of variables now leads to the *discrete modes*

$$\beta_n(x, t) = e^{2\pi i(\frac{nx}{L} + \omega_n t)} + c.c., \quad (2\pi\omega_n)^2 = (\frac{2\pi n}{L})^2[p^2(\frac{2\pi n}{L})^2 - 2pqA^2]. \quad (13)$$

While this is analogous to equation (9), there is a very important difference: *depending on the values of p, q, A, L , there may not be even one unstable mode*. Indeed, $\omega_0 = 0$ and for any $0 \neq n \in \mathbb{Z}$ we have

$$\omega_n^2 < 0 \iff L > \frac{2\pi|n|}{A} \sqrt{\frac{p}{2q}}. \quad (14)$$

That is, the computational domain L has to be larger than

$$L_c := \frac{2\pi\sqrt{p}}{A\sqrt{2q}} \quad (15)$$

otherwise the MI is *completely suppressed*. Observe moreover that the lengthscale L_c does not depend on the initial inhomogeneity $\delta_0(x)$, and becomes larger when the nonlinearity becomes weaker (i.e. when $q, A > 0$ decrease). For water waves with typical wavenumber k_0 (equivalently typical wavelength $\lambda_0 = 2\pi/k_0$), the coefficients are $p = \sqrt{g}/(8k_0^{3/2})$, $q = \sqrt{g}k_0^{5/2}/2$ [20] leading to

$$L_c = \frac{1}{4\pi\sqrt{2}} \frac{\lambda_0^2}{A}. \quad (16)$$

Note that the waves that would be dangerous for ships in the ocean and carry most of the surface wave energy have wavelengths in the hundreds of meters.

2.3 Numerical investigation

In what follows we present numerical solutions of the problem

$$\begin{aligned} i\partial_t u + p\Delta u + q|u|^2 u &= 0, & u(x, 0) &= A(1 + \delta_j(x)) \\ u(-\frac{L}{2}, t) &= u(\frac{L}{2}, t), & \partial_x u(-\frac{L}{2}, t) &= \partial_x u(\frac{L}{2}, t), \end{aligned} \quad (17)$$

for the initial inhomogeneities

$$\begin{aligned} \delta_1(x) &= A(1 + 0.03 \cdot \operatorname{sech}(15x) \cos(5x)), & \delta_2(x) &= A(1 + 0.03 \cdot \operatorname{sech}(15x)), \\ \delta_3(x) &= A(1 + 0.03 \cdot e^{-3x^2}), & \delta_4(x) &= A(1 + 0.03 \cdot e^{-x^4}), & \delta_5(x) &= A(1 + 0.06 \cdot x \cdot e^{-x^4}), \end{aligned} \quad (18)$$

and $p = q = A = 1$. The bifurcation length in this case is $L_c \approx 4.45$; the solutions are computed for $L = 0.98L_c$, $L = 1.3L_c$, $L = 3L_c$ and $L = 10L_c$. The computation time is $t \in [0, 10]$. The numerical

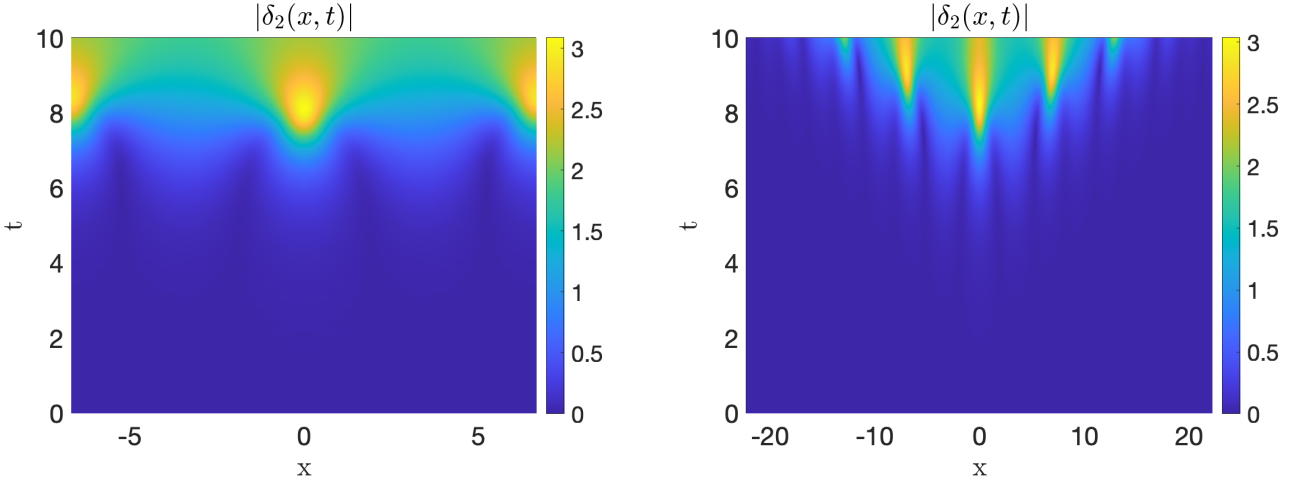


Figure 2: Space-time plot of the inhomogeneity $|\delta_2|$ when propagated on intervals of different length L according to equations (17) – (19). The bifurcation length L_c is reported in equation (15). **Left:** $L = 3L_c$. **Right:** $L = 10L_c$.

	$N = 0.98$	$N = 1.3$	$N = 3$	$N = 10$
$j = 1$	0.0359	2.59	3.08	3.03
$j = 2$	0.0393	2.59	3.09	3.03
$j = 3$	0.149	2.65	3.17	3.12
$j = 4$	0.25	2.69	3.22	3.18
$j = 5$	0.03	2.57	3.05	2.96

Table 1: Maximum value of the inhomogeneity $\max_{x,t} |\delta(x,t)|$ for $x \in [-L/2, L/2]$ and $t \in [0, 10]$, with $L = NL_c$ (cf. equation (15)) and initial condition $\delta_j(x, 0)$ (cf. equation (18)).

scheme used is a relaxation in time with second-order finite differences in space, and it satisfies mass and energy conservation on the discrete level [8, 9]. The inhomogeneity $\delta(x, t)$ for $t \in [0, 10]$ is defined as

$$\delta(x, t) := (u(x, t) - Ae^{iqA^2 t}) \frac{1}{A} e^{-iqA^2 t} \quad (19)$$

consistently with equation (4). Numerical results can be found in Figures 1 and 2, as well as in Table 1.

The initial inhomogeneities δ_1 and δ_2 are localized sech bumps, and are quite similar to each other. δ_3 and δ_4 are also bumps with different profiles, and δ_5 is a localised wave. In Table 1 the maximum moduli of the inhomogeneities are recorded when propagated on intervals of different lengths. There is a clear confirmation of the abrupt bifurcation, namely an abrupt change in behaviour from $L = 0.98L_c$ to $L = 1.3L_c$.

On the larger intervals $L = 3L_c$, $L = 10L_c$, coherent structures emerge. These are a sign that the MI has been resolved in a manner qualitatively similar to what would happen on the real line (that is, until the structures reach close to the boundary of the computational domain). These structures all involve localised maxima supported on neighbourhoods of size roughly L_c each. In the larger domain, the well-known space-time cone [11, 12, 10] is clearly visible.

Crucially, when the length of the domain becomes $L < L_c$, we don't merely see a periodised or slightly off version of the cone, but something completely different: the amplification is small or non-existent and there is no spatial pattern at all, see left graph in Figure 1. Indeed, for all initial data, when $L = 0.98L_c$, the inhomogeneity initially disperses rapidly and then slowly grows in homogeneous way over the whole computational domain.

3 Stability analysis for stochastic sea states

Following [1, 3], we can derive the second moment equation

$$i\partial_t R + \frac{p}{2} (\Delta_x - \Delta_y) R + qR(x, y, t) [R(x, x, t) - R(y, y, t)] = 0 \quad (20)$$

for the two-space autocorrelation,

$$R = R(x, y, t) = E[u(x, t)\bar{u}(y, t)]. \quad (21)$$

A standard gaussian closure, inspired by the linear theory of water waves, is used to arrive to equation (20). Moreover, by assuming that the wavefield is quasi-homogeneous,

$$R(x, y, t) = \Gamma(x - y) + \rho(x, y, t), \quad \rho(x, y, 0) = o(1), \quad (22)$$

we derive the Alber equation for the evolution of the inhomogeneous part,

$$i\partial_t \rho + \frac{p}{2} (\Delta_x - \Delta_y) \rho + q [\Gamma(x - y) + \rho(x, y, t)] [\rho(x, x, t) - \rho(y, y, t)] = 0. \quad (23)$$

Observe that whether the starting point is the real line, equation (1), or an interval of length L , equation (11), equation (23) still applies – equipped with the appropriate boundary conditions in each case. Moreover, in the periodic boundary conditions case, these are inherited by the second moments; in particular we can express moments in terms of Fourier series on the interval $[-\frac{L}{2}, \frac{L}{2}]$,

$$\Gamma(y) = \sum_{n \in \mathbb{Z}} P_n e^{2\pi i \frac{ny}{L}}, \quad \rho(x, y, t) = \sum_{k, l \in \mathbb{Z}} r_{k,l}(t) e^{2\pi i \frac{kx+ly}{L}}. \quad (24)$$

So by linearising (dropping terms of $O(\rho^2)$) and expressing everything in terms of Fourier coefficients we have

$$\begin{aligned} & i \sum_{k, l \in \mathbb{Z}} \partial_t r_{k,l}(t) e^{2\pi i \frac{kx+ly}{L}} + \frac{p}{2} \sum_{k, l \in \mathbb{Z}} r_{k,l}(t) ((2\pi i \frac{k}{L})^2 - (2\pi i \frac{l}{L})^2) e^{2\pi i \frac{kx+ly}{L}} + \\ & + q \left(\sum_{n \in \mathbb{Z}} P_n e^{2\pi i \frac{n(x-y)}{L}} \right) \left(\sum_{k, l \in \mathbb{Z}} r_{k,l}(t) \left[e^{2\pi i \frac{k+l}{L}x} - e^{2\pi i \frac{k+l}{L}y} \right] \right) = 0. \end{aligned} \quad (25)$$

By taking the inner product with $e^{2\pi i \frac{k'x+l'y}{L}}$ (and suppressing the primes) we obtain

$$\partial_t r_{k,l}(t) + i \frac{2\pi^2 p}{L^2} r_{k,l}(t) (k - l)(k + l) - iq [P_{-l} - P_k] \sum_{K \in \mathbb{Z}} r_{K,k+l-K}(t) = 0 \quad (26)$$

which in mild form becomes

$$r_{k,l}(t) = e^{-ip \frac{2\pi^2 (k+l)(k-l)}{L^2} t} r_{k,l}(0) + \int_{\tau=0}^t e^{-ip \frac{2\pi^2 (k+l)(k-l)}{L^2} (t-\tau)} iq [P_{-l} - P_k] \sum_{K \in \mathbb{Z}} r_{K,k+l-K}(\tau) d\tau. \quad (27)$$

At this point denote

$$f(\xi, t) = \sum_{K \in \mathbb{Z}} r_{K,\xi-K}(\tau), \quad \xi \in \mathbb{Z}; \quad (28)$$

this corresponds to the ξ 'th Fourier coefficients of the inhomogeneous part of the position density $|u(x, t)|^2$. The point is that if we know $f(\xi, t)$ then $r_{k,l}(t)$ can be computed by substitution in equation (27), i.e. $f(\xi, t)$ is what really drives the problem. Now we will extract from equation (27) a closed equation for $f(\xi, t)$. To that end, set $k + l = \xi$, $l = \xi - k$, $k - l = 2k - \xi$; thus, equation (27) becomes

$$r_{k,\xi-k}(t) = e^{-ip \frac{2\pi^2 \xi (2k-\xi)}{L^2} t} r_{k,\xi-k}(0) + \int_{\tau=0}^t e^{-ip \frac{2\pi^2 \xi (2k-\xi)}{L^2} (t-\tau)} iq [P_{k-\xi} - P_k] \sum_{K \in \mathbb{Z}} r_{K,\xi-K}(\tau) d\tau. \quad (29)$$

By summing equation (29) in k it follows that

$$f(\xi, t) = \underbrace{\sum_k e^{-ip\frac{2\pi^2\xi(2k-\xi)}{L^2}t} r_{k,\xi-k}(0)}_{\phi(\xi,t)} + \int_{\tau=0}^t \left[\underbrace{\sum_k e^{-ip\frac{2\pi^2\xi(2k-\xi)}{L^2}(t-\tau)} iq(P_{k-\xi} - P_k)}_{h(\xi,t-\tau)} \right] f(\xi, \tau) d\tau \quad (30)$$

Now by Laplace transform this leads to

$$\tilde{f}(\xi, \omega) = \tilde{\phi}(\xi, \omega) + \tilde{h}(\xi, \omega) \tilde{f}(\xi, \omega) \implies \tilde{f}(\xi, \omega) = \frac{\tilde{\phi}(\xi, \omega)}{1 - \tilde{h}(\xi, \omega)} \quad (31)$$

So in complete analogy to the real line case [3] we obtain a Penrose-type stability condition, namely

$$\inf_{\substack{\text{Re } \omega > 0 \\ \xi \in \mathbb{R}}} |1 - \tilde{h}(\xi, \omega)| = \kappa > 0. \quad (32)$$

In terms of working out explicitly the function \tilde{h} , observe that for any ω with $\text{Re } \omega > 0$ we have

$$\tilde{h}(\xi, \omega) = \int_{t=0}^{\infty} e^{-\omega t} \left[\sum_{k \in \mathbb{Z}} e^{-ip\frac{2\pi^2\xi(2k-\xi)}{L^2}t} iq(P_{k-\xi} - P_k) \right] dt = iq \sum_{k \in \mathbb{Z}} \frac{P_{k-\xi} - P_k}{\omega + ip\frac{2\pi^2\xi(2k-\xi)}{L^2}} \quad (33)$$

It is worth noting that this condition can be seen as a discretization of the known Penrose stability condition on the real line when $P_n = \frac{1}{L}S(\frac{n}{L})$ for the continuous power spectrum $S(k)$. (This can be readily seen by following the same steps as here, starting from equation (23) on the real line and using continuous Fourier transforms in the place of Fourier series.) Thus the linear stability characteristics of the problem (11) do converge as $L \rightarrow \infty$, but the question is how large must L get before the stability behavior effectively settles.

For practical applications it suffices to work out a slightly weaker sufficient condition for instability. Namely, the wavenumber $\xi \in \mathbb{Z}$ is unstable if

$$\exists \omega \text{ with } \text{Re } \omega > 0 \quad : \quad \tilde{h}(\xi, \omega) = 1. \quad (34)$$

For the case of a plane wave, $P_n = C\delta_{n,n_0}$, it is easy to see that this leads to a result equivalent to equation (15). More generally however, equation (34) is a system of two nonlinear equations (real and imaginary parts) in three unknowns $(\xi, \text{Re } \omega, \text{Im } \omega)$, and solving it is not straightforward. Still, it is relatively easy to investigate whether it has any solutions at all. Let us fix the value of ξ as a parameter and consider \tilde{h}_ξ as a function of ω alone. One observes that \tilde{h}_ξ is holomorphic on the right half plane; thus it satisfies the argument principle: if the curve \mathcal{D} winds around ω , then the curve $\tilde{h}_\xi(\mathcal{D})$ will wind around $\tilde{h}_\xi(\omega)$. So now let us consider a Nyquist contour \mathcal{D} , i.e. a D -shaped contour consisting of the line $\{\varepsilon + is\}_{s=-\frac{1}{\varepsilon}}^{\frac{1}{\varepsilon}}$ and the arc $\{\frac{1}{\varepsilon}(\cos\theta + i \sin\theta)\}_{\theta=\arccos\varepsilon^2}^{-\arccos\varepsilon^2}$. (This encloses the right half of the disk with center 0 and radius $\frac{1}{\varepsilon}$, except a strip of width ε next to the imaginary axis.) The advantage is that $\tilde{h}_\xi(\mathcal{D})$ can be directly computed, and $\tilde{h}_\xi(\omega) = 1$, if a solution of the instability condition (34) exists. So by plotting the curve $\tilde{h}_\xi(\mathcal{D})$ we can directly determine whether the wavenumber ξ is unstable (in which case $\tilde{h}_\xi(\mathcal{D})$ winds around 1) or not.

We can use this method to investigate e.g. the behaviour of a narrow spectrum that is nevertheless not a plane wave: let us take

$$P_n = C \left(\frac{1}{2}\delta_{n,-1} + \delta_{n,0} + \frac{1}{2}\delta_{n,1} \right) \quad (35)$$

and focus on $\xi = 1$, i.e. on whether there exists at least one unstable wavenumber. We will use the water waves scaling $p = \sqrt{g}/(8k_0^{3/2})$, $q = \sqrt{g}k_0^{5/2}/2$ [20], and set different values of L measured in wavelengths

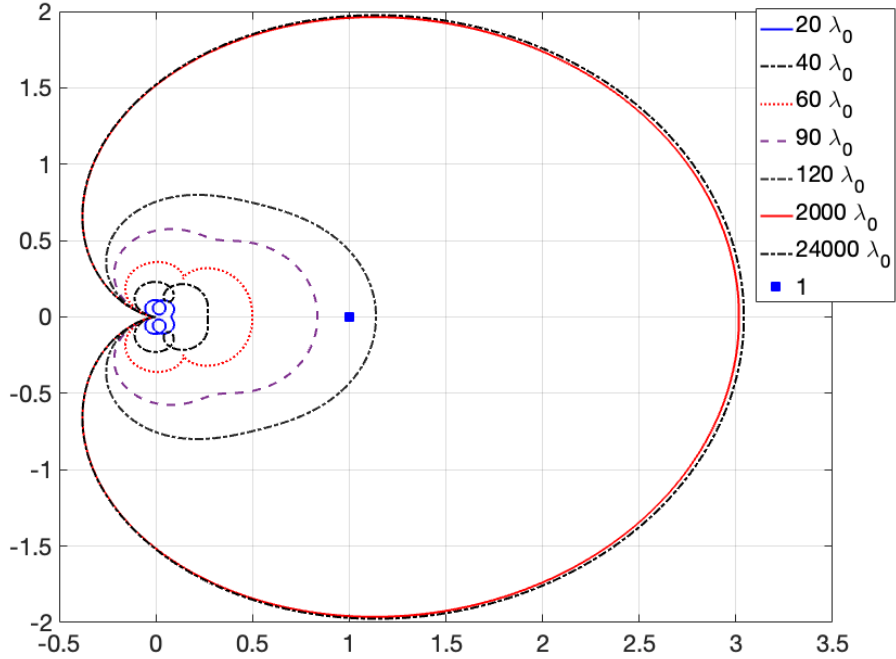


Figure 3: Stability curves for $\xi = 1$ and different lengths L of the interval used. Note that the two largest lines are very close, even though the correspond to very different values of L , i.e. the stability characteristics of the problem have settled.

$\lambda_0 = \frac{2\pi}{k_0}$ in the expression (33) for \tilde{h}_ξ . The resulting curves (the images under \tilde{h}_ξ of the Nyquist contour) are shown in Figure 3.

It is clearly seen that the linear stability characteristics of the problem converge as L grows, but not until L is in the high hundreds of wavelengths. Moreover, in this particular example, instability first kicks in for L between 90 and 120 wavelengths.

4 Conclusions

In this work we investigate the fundamental scaling of the MI on a bounded interval for the periodized NLS with the water waves normalization. A lengthscale of $L_c = O(\lambda_0^2)$ is found to be required before linear instability is present; this translates to hundreds of wavelengths for water waves problems. In plane waves, where the result is very clear cut, it is seen that less nonlinear problems (smaller q, A in equation (3)) require larger domains for the MI to manifest. In other words, the rule of thumb is that less unstable problems require larger computational domains for the MI to be present. With that in mind, it is worth noting that water waves problems with realistic power spectra are either stable or barely unstable [3, 17, 26]. Thus, it is natural to require very large domains to see the instability for unstable spectra. This seems to be confirmed by the numerical investigation of the stability condition for a model narrow spectrum in Section 3, and by the works that did detect the onset of MI [23, 26, 5].

The second moments analysis of Section 3 is not meant to substitute detailed, phase-resolved numerical investigation of stochastic wavefields. On the contrary, it can help to calibrate such simulations correctly, reminding that the MI is a non-local effect and estimating the size of computational domain required in order to simulate it.

More broadly, the validity of the NLS and any analysis built on it are often challenged in the context of water waves, citing broad spectra, two dimensional problems etc as limitations. For quasi-unidirectional

problems, we must note that the goal here is simply to obtain a fundamental scaling for the size of the computational domain needed to resolve the MI, not a detailed simulation of water waves. Moreover, recent work has shown that the MI for the fully nonlinear water waves problem is accurately captured by the NLS [7, 21]. Thus, we expect the main finding to be valid for real-world water waves in quasi-unidirectional seas; of course further numerical simulations on large computational domains are required in order to conclusively test this. Extensions to crossing seas [18, 4] are in principle possible and a natural next step.

References

- [1] I. E. ALBER, *The Effects of Randomness on the Stability of Two-Dimensional Surface Wavetrains*, Proceedings of the Royal Society A: Mathematical, Physical and Engineering Sciences, 363 (1978), pp. 525–546.
- [2] D. ANDRADE AND M. STIASSNIE, *New solutions of the C.S.Y. equation reveal increases in freak wave occurrence*, Wave Motion, 97 (2020), p. 102581.
- [3] A. ATHANASSOULIS, G. ATHANASSOULIS, M. PTASHNYK, AND T. SAPSIS, *Strong solutions for the Alber equation and stability of unidirectional wave spectra*, Kinetic and Related Models, 13 (2020), pp. 703–737.
- [4] A. ATHANASSOULIS AND O. GRAMSTAD, *Modelling of ocean waves with the alber equation: Application to non-parametric spectra and generalisation to crossing seas*, Fluids, 6 (2021), p. 291.
- [5] A. G. ATHANASSOULIS, *Phase Resolved Simulation of the Landau-Alber Stability Bifurcation*, Fluids, 8 (2023).
- [6] F. BARONIO, S. CHEN, P. GRELU, S. WABNITZ, AND M. CONFORTI, *Baseband modulation instability as the origin of rogue waves*, Physical Review A - Atomic, Molecular, and Optical Physics, 91 (2015), p. 033804.
- [7] M. BERTI, A. MASPERO, AND P. VENTURA, *Full description of Benjamin-Feir instability of stokes waves in deep water*, Inventiones Mathematicae, 230 (2022), pp. 651–711.
- [8] C. BESSE, *A relaxation scheme for the nonlinear Schrödinger equation*, SIAM Journal on Numerical Analysis, 42 (2004), pp. 934–952.
- [9] C. BESSE, S. DESCOMBES, G. DUJARDIN, AND I. LACROIX-VIOLET, *Energy-preserving methods for nonlinear Schrödinger equations*, IMA Journal of Numerical Analysis, 41 (2021), pp. 618–653.
- [10] G. BIONDINI, S. LI, D. MANTZAVINOS, AND S. TRILLO, *Universal Behavior of Modulationally Unstable Media*, SIAM Review, 60 (2018), pp. 888–908.
- [11] G. BIONDINI AND D. MANTZAVINOS, *Universal Nature of the Nonlinear Stage of Modulational Instability*, Physical Review Letters, 116 (2016), pp. 1–5.
- [12] ——, *Long-Time Asymptotics for the Focusing Nonlinear Schrödinger Equation with Nonzero Boundary Conditions at Infinity and Asymptotic Stage of Modulational Instability*, Communications on Pure and Applied Mathematics, 70 (2017), pp. 2300–2365.
- [13] D. R. CRAWFORD, P. G. SAFFMAN, AND H. C. YUEN, *Evolution of a random inhomogeneous field of nonlinear deep-water gravity waves*, Wave Motion, 2 (1980), pp. 1–16.
- [14] K. DYSTHE, H. E. KROGSTAD, AND P. MÜLLER, *Oceanic Rogue Waves*, Annual Review of Fluid Mechanics, 40 (2008), pp. 287–310.

- [15] F. FEDELE, J. BRENNAN, S. P. D. LEÓN, J. DUDLEY, AND F. DIAS, *Real world ocean rogue waves explained without the modulational instability*, Scientific Reports, 6 (2016), pp. 1–11.
- [16] C. GALLO, *Schrödinger group on Zhidkov spaces*, Advances in Differential Equations, 9 (2004), pp. 509–538.
- [17] O. GRAMSTAD, *Modulational instability in Jonswap sea states using the alber equation*, 2017.
- [18] O. GRAMSTAD, E. BITNER-GREGERSEN, K. TRULSEN, AND J. C. N. BORGE, *Modulational instability and rogue waves in crossing sea states*, Journal of Physical Oceanography, 48 (2018), pp. 1317–1331.
- [19] P. A. E. M. JANSSEN, *Nonlinear Four-Wave Interactions and Freak Waves*, Journal of Physical Oceanography, 33 (2003), pp. 863–884.
- [20] C. C. MEI, M. STIASSNIE, AND D. K.-P. YUE, *Theory and Applications of Ocean Surface Waves*, vol. 23, World Scientific, 7 2005.
- [21] H. Q. NGUYEN AND W. A. STRAUSS, *Proof of Modulational Instability of Stokes Waves in Deep Water*, Communications on Pure and Applied Mathematics, 76 (2023), pp. 1035–1084.
- [22] M. OLAGNON AND M. PREVOSTO, eds., *Rogue Waves 2004*, Ifremer, 2004.
- [23] M. ONORATO, A. OSBORNE, R. FEDELE, AND M. SERIO, *Landau damping and coherent structures in narrow-banded 1 + 1 deep water gravity waves*, Physical Review E, 67 (2003), p. 046305.
- [24] M. ONORATO, A. R. OSBORNE, AND M. SERIO, *Modulational Instability in Crossing Sea States: A Possible Mechanism for the Formation of Freak Waves*, Physical Review Letters, 96 (2006), p. 014503.
- [25] M. ONORATO, S. RESIDORI, U. BORTOLOZZO, A. MONTINA, AND F. T. ARECCHI, *Rogue waves and their generating mechanisms in different physical contexts*, Physics Reports, 528 (2013), pp. 47–89.
- [26] A. RIBAL, A. V. BABANIN, I. YOUNG, A. TOFFOLI, AND M. STIASSNIE, *Recurrent solutions of the Alber equation initialized by Joint North Sea Wave Project spectra*, Journal of Fluid Mechanics, 719 (2013), pp. 314–344.
- [27] A. V. SLUNYAEV, D. E. PELINOVSKY, AND E. N. PELINOVSKY, *Rogue waves in the sea: observations, physics and mathematics*, Physics-Uspekhi, (2021).
- [28] K. TRULSEN, *Rogue Waves in the Ocean, the Role of Modulational Instability, and Abrupt Changes of Environmental Conditions that Can Provoke Non Equilibrium Wave Dynamics*, (2018), pp. 239–247.
- [29] V. E. ZAKHAROV AND L. A. OSTROVSKY, *Modulation instability: The beginning*, Physica D: Nonlinear Phenomena, 238 (2009), pp. 540–548.
- [30] P. ZHIDKOV, *The Cauchy problem for the nonlinear Schrödinger equation*, 1987.

Acknowledgment. The authors would like to thank Prof. G. A. Athanassoulis, Prof. T. Sapsis, Dr. O. Gramstad and Dr. T. Tang for helpful discussions.

Declaration of interests: The authors report no conflict of interest.